PHYSICAL REVIEW B VOLUME 22, NUMBER 10 15 NOVEMBER 1980

# Energy-dependent electron-energy-loss spectroscopy: Application to the surface and bulk electronic structure of MgO

Victor E. Henrich,* G. Dresselhaus,† and H. J. Zeiger
*Lincoln Laboratory, Massachusetts Institute of Technology, Lexington, Massachusetts 02173*
(Received 23 May 1980)

The various effects that can occur when the primary electron energy, $E_p$, is varied in a reflection-energy-loss experiment are considered. For $E_p \geq 100$ eV, the dominant effect is an increase of the electron mean free path with increasing $E_p$. By performing energy-loss measurements with 100 eV $\leq E_p \leq$ 2000 eV, it is possible to unambiguously separate bulk and surface features in loss spectra. That technique has been applied to the MgO (100) surface, and both Mg intraionic and O-to-Mg interionic transitions have been studied. The former transitions are found to agree well with the excited-state spectra of free $Mg^{2+}$ ions, while the latter agree more closely with itinerant-electron calculations of MgO. Intrinsic surface-state transitions are seen in both $Mg^{2+}$ and O-to-Mg spectra. The Mg core-level surface-state spectra can be explained by Stark splitting of the surface $Mg^{2+}$ levels in the intense electric fields at the crystal surface. The surface-state structure seen in O-to-Mg loss spectra agrees with discrete variational $X\alpha$ calculations of the MgO (100) surface and disagrees with linear combination of atomic orbitals calculations of the same surface. A low-energy-loss peak, possibly associated with surface defects, is seen on some surfaces; the exact nature of the surface defects involved is not yet clear.

## I. INTRODUCTION

Ever since the pioneering work of Rudberg[1] in 1930 on reflection electron-energy-loss spectroscopy (ELS), experimentalists have varied the energy of the incident (primary) electron beam, $E_p$, in order to assist in interpreting the spectra. Since the energy-loss features in a secondary-electron spectrum $n(E)$ are always located at the same energy below $E_p$, varying $E_p$ allows one to separate loss features from other structures in $n(E)$, such as Auger peaks, whose kinetic energy is independent of $E_p$. In fact, a common method of obtaining energy-loss spectra free of Auger peaks, and the method used in the work reported here, is to apply a small modulation voltage to $E_p$, with no modulation of the electron spectrometer, and synchronously detect the output of the spectrometer. Another reason for varying $E_p$ is to separate different types of transitions seen in the spectra by means of the different energy dependences of their transition probabilities. This effect is generally strongest for $E_p \lesssim 100$ eV, and it has been used by several authors[2-4] to interpret the origin of energy-loss peaks.

The energy dependence of the mean free path $\lambda(E)$ of electrons in solids[5] can also be used to separate surface and bulk transitions in energy-loss spectra. This effect can be used most effectively for $E_p \gtrsim 100$ eV where other energy-dependent effects are relatively small. One of the first uses of $\lambda(E)$ for this purpose was by Powell and Swan[6] to identify surface plasmons on aluminum. Many experimentalists have made qualitative use of this effect since then.[7]

We have recently used the energy dependence of $\lambda(E)$ to study surface and bulk excitonic core-level transitions in MgO; a brief report of some of that work has been published previously.[8] In this paper we report additional measurements of intraionic core-level spectra as well as interionic (or interband) spectra involving both Mg and O ions. The surface and bulk transitions are separated by the method described above, and the transitions are then compared to both ionic and band models of the electronic structure of MgO. In Sec. II we will outline the theoretical considerations relevant to energy-dependent electron-energy-loss spectroscopy. The experimental methods that we have used will be discussed in Sec. III. In Sec. IV the method will be applied to core-level excitations of the $Mg^{++}$ ion in MgO, and we will review the model for the origin of the excitonic surface states seen in these spectra. The energy-loss spectra for interionic O-to-Mg transitions will be presented and discussed in Sec. V. Section VI will consider defect surface states on MgO.

## II. THEORETICAL CONSIDERATIONS

Electron-energy-loss experiments on solids can be performed by transmission of high-energy electrons (10–100 keV) through thin samples[9] (roughly 100–1000 Å) or by reflection of lower-energy electrons ($\lesssim$2 keV) from thick samples. In transmission the energy loss $\Delta E$ is always small compared to $E_p$, and the electrons generally undergo only one scattering event. The scattering cross section is then well described by[9]

$$\frac{d^2\sigma}{d(\Delta E)d\Omega} = \frac{m}{\pi^2 n a_0 \hbar^2 (\Delta k^2)} \operatorname{Im}\left(\frac{-1}{\epsilon(\Delta E)}\right), \quad (1)$$

 © 1980 The American Physical Society

where $\Delta k$ is the momentum loss during scattering, $m$ is the electron mass, $n$ is the number of electrons per volume participating in the loss process, $a_0$ is the Bohr radius, and $\epsilon$ is the longitudinal dielectric constant of the solid. There is no interesting dependence of the loss spectrum on $E_p$ in this regime, and $E_p$ need only be kept large enough that the probability of multiple scattering in the sample is low.

In the reflection mode, only electrons that have been scattered back out of the sample are detected. The electrons must thus undergo either large-angle inelastic scattering or small-angle inelastic scattering preceded or followed by large-angle elastic diffraction. In addition, the assumptions that $\Delta E \ll E_k$ and $\Delta k \ll k_p$, implicit in Eq. (1),[9] may not be met for low incident-electron energies or for loss processes involving atomic core levels. When the presence of the surface is explicitly taken into account,[10] but the other assumptions implicit in Eq. (1) are retained (e.g., validity of the Born approximation), it is found that the loss function is proportional to $\mathrm{Im}\{-1/[\epsilon(\Delta E)+1]\}$. For free-electron metals this shifts the plasma frequency down to that of the surface plasmon. For interband transitions, $\mathrm{Im}(-1/\epsilon)$ and $\mathrm{Im}[-1/(\epsilon+1)]$ generally differ only in small shifts of the energies of the loss peaks. To determine the role of the incident-electron energy in the energy-loss process, the various aspects of the loss process will be considered separately.

### A. Electron-atom and electron-ion interactions

The incident-electron-energy dependence of most low-energy inelastic scattering processes in solids has not been investigated either experimentally or theoretically. Inelastic scattering of electrons by free atoms, ions, and molecules in gases has been studied extensively, however, and a comprehensive review is available in the books by Massey and Burhop.[11,12] Since the same basic interactions govern electron scattering in both cases, we can get a good idea of the effects to be expected in solids from the results obtained on gases. This general approach has been used by Powell[13] in calculations of the mean free paths of electrons in solids. The effects that cannot be generalized from free-atom scattering are those which result from the high density of atoms in solids, such as collective excitations (plasmons) and the dispersion produced by banding; those must be considered separately.

The basic form of the excitation function (or cross section), $f(E_p)$ vs $E_p$, for intra-atomic excitations is perhaps best illustrated for the case of He atoms (see Fig. 4.21 of Ref. 11). Two general types of curves are observed. Transitions that are allowed by the optical (dipole) selection rules have excitation functions that rise from zero below the threshold energy for the excitation to a maximum at three to four times the threshold energy and then fall relatively slowly at higher energies $[f(E_p)_{\text{allowed}} \sim \ln(E_p)/E_p]$. The excitation functions for optically forbidden transitions (which are allowed in electron excitation, however) rise more rapidly to a sharp peak at about twice the threshold energy and then fall rapidly with increasing energy $[f(E_p)_{\text{forbidden}} \sim 1/E_p]$. Data are available on inelastic electron scattering from a large number of other atoms[11] and, while it can be more complex in the vicinity of the threshold, particularly for heavy atoms, the behavior of $f(E_p)$ above its maximum almost always lies somewhere between the two cases for He. Data on interatomic excited states in compound molecules by electron impact[12] also exhibit excitation functions similar to those for atoms.

The above considerations have been applied to energy-loss measurements on Ge and GaAs by Ludeke and Koma.[2] They varied $E_p$ between 50 and 100 eV and attributed peaks whose amplitude increased with decreasing $E_p$ as arising from dipole-forbidden transitions. Ritsko *et al.*[3] applied similar considerations to energy-loss spectra from tetrathiafulvalenium-tetracyanoquinodimethane (TTF-TCNQ). Rubloff[4] has considered the effects of selection rules on energy-loss spectra for a variety of materials.

One interesting deviation from the normal threshold behavior in electron-atom collisions has been observed in some heavy atoms.[14] The Auger-electron yields for the $N_{6,7}O_{4,5}O_{4,5}$ transitions in Au, Bi, and Pb are found to have apparent thresholds that are 60–70 eV higher than those to be expected from the energy differences between the corresponding levels. Such a delayed threshold is also seen in the x-ray absorption spectra of these levels.[14] The effect is believed to arise from the large angular momentum of the $4f$ initial state and the correspondingly large angular momentum of the emitted electron. It should be readily apparent in energy-dependent electron-energy-loss spectra since the loss peaks corresponding to those transitions would appear for larger incident-electron energies than would other peaks in that region of the loss spectrum.

### B. Plasmon-electron interactions

The coupling of electrons to bulk and surface plasma oscillations in the energy region of interest for reflection energy-loss measurements has been treated theoretically by several authors.[15,16] The

results of the calculations show that the electrons near the surface excite mainly surface plasmons, while those deeper inside have a higher probability of exciting bulk plasmons. As the electron energy is increased, the greater range of the electrons results in the creation of a smaller fraction of surface plasmons compared to bulk plasmons. (The actual calculations are more complex than the above description implies,[16] but the net result is the same.) This effect has been observed by numerous workers,[7] one of the first being Powell and Swan[6] in reflection energy-loss measurements on aluminum for $760 \leq E_p \leq 2020$ eV.

### C. Diffraction

Since the electrons that are analyzed in a reflection energy-loss experiment have undergone large-angle scattering, most of them have suffered at least one elastic diffraction. For polycrystalline or amorphous samples or samples with disordered surfaces (e.g., many single crystals after cleaning by ion bombardment), diffraction will play essentially no role, since any detection geometry will see an average over many diffraction conditions. Crystals with nearly perfect surfaces, however, exhibit strong electron diffraction effects [e.g., distinct low-energy electron diffraction (LEED) patterns], and these effects can give different energy-loss spectra for different spectrometer geometries or primary-electron energies. For example, changes in the amplitude of an energy-loss spectrum can occur when LEED beams enter or leave the acceptance region of the spectrometer. It is therefore difficult to compare the amplitude of energy-loss spectra taken at different primary energies. Relative amplitudes within a single spectrum can still be compared, however, if $E_p$ is fixed during each spectrum. However, if the electron kinetic energy that is analyzed is held constant and $E_p$ is varied, as is sometimes done in order to eliminate Auger features from the energy-loss spectra, spurious structure can occur when diffracted beams enter or leave the analyzer acceptance aperture.

### D. Mean-free-path and surface-state effects

The sum of all energy-loss processes gives rise to an energy-dependent total mean free path $\lambda(E)$ for electrons in solids. This mean free path is used in the usual manner to determine the intensity $I(z)$ of the incident beam at the site of the energy-loss process:

$$I(z) = I_0 e^{-z \sec\theta/\lambda(E_p)}, \tag{2}$$

where $I_0$ is the intensity of the incident beam at the surface, $z$ is the distance of the scattering site below the surface, and $\theta$ is the angle between the direction of the electron beam in the sample and the inward normal to the surface. A similar expression is applied to the attenuation of scattered electrons leaving the sample. Measurements of $\lambda(E)$ have been made by several techniques on a variety of materials, and Fig. 1 shows one compilation of some of the data.[5] The mean free path has a minimum in the vicinity of $E = 20$–$100$ eV and increases roughly as $\sqrt{E}$ for higher energies. For energy-loss experiments performed with incident electrons between 100 and 2000 eV, as in the present work, $\lambda(E)$ can vary between 3–5 Å and 20–30 Å. The effective depth sampled can thus be changed from about 1 lattice constant for $E_p \sim 100$ eV to 5–10 lattice constants for $E_p \sim 2000$ eV.

This ability to change the depth sampled makes it possible to separate surface and bulk contributions to the energy-loss spectra. Electronic surface states are usually localized to the first few angstroms of the surface and will thus make a stronger contribution to the spectra at low energies than at high energies. For example, assume that the atoms in a layer of thickness $d$ at the surface of a sample have electronic properties different from those of the bulk. For an electron beam of energy $E_p$ and intensity $I_0$ incident normal to the surface, the intensity at a distance $z$ below the surface $I(z)$ is given by Eq. (2) with $\theta = 0°$. If we assume that the electrons scattered back out of the sample also move normal to the surface and that the primary and scattered electron energies are close enough that we can use the same mean free path for both, then the intensity of electrons scattered at a depth $z$ that get out of the sample $I'(z)$ is

$$I'(z) = C\,|M(E_p)|^2 I_0 e^{-2z/\lambda(E_p)}, \tag{3}$$

where $C$ is a constant and $M(E_p)$ is the matrix element giving the probability of electrons exciting a particular transition. The total intensity $I'_s$ due

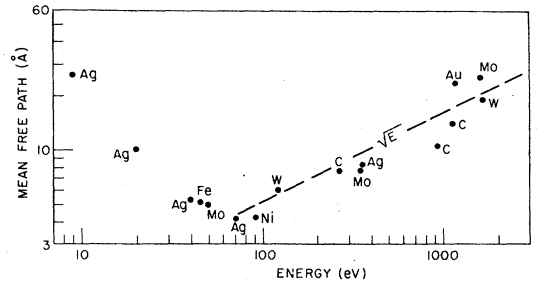


FIG. 1. Mean free path of electrons in various materials versus kinetic energy (after J. C. Tracy) (from Ref. 5).

to the surface region is then

$$I_s' = C|M_s(E_p)|^2 I_0 \int_0^d e^{-2z/\lambda(E_p)}\,dz\,, \tag{4}$$

where $M_s(E_p)$ is the matrix element for a surface-state transition. The intensity $I_B'$ due to the bulk is

$$I_B' = C|M_B(E_p)|^2 I_0 \int_d^\infty e^{-2z/\lambda(E_p)}dz\,, \tag{5}$$

where $M_B(E_p)$ is the corresponding bulk-matrix element. The relative intensity of the surface and bulk energy-loss features is thus

$$\frac{I_s'}{I_B'} = \frac{|M_s(E_p)|^2}{|M_B(E_p)|^2}\,\frac{(1-e^{-2d/\lambda(E_p)})}{e^{-2d/\lambda(E_p)}}\,. \tag{6}$$

If we assume that $M_s(E_p) \approx M_B(E_p)$ and take $d = 2$ Å (top layer of atoms), then the amplitude of surface-to-bulk loss features is found from Eq. (6) to decrease by an order of magnitude as $\lambda(E_p)$ varies from 4 to 25 Å.

In the energy-loss experiments reported in this paper, the primary-electron energy $E_p$ was varied between 100 and 2000 eV. Based on the considerations given above, the largest contribution to the energy dependence of features in the loss spectrum would be expected to arise from changes in the electron mean free path. We have interpreted our data based on this premise, except where noted otherwise.

## III. EXPERIMENTAL METHODS

If meaningful comparisons are to be made between energy-loss spectra taken at different incident-electron energies, no other parameters in the experiment can change. In particular, the energy profile of the incident-electron beam and the resolution of the electron spectrometer must be independent of energy. The latter criterion can be fulfilled by electron spectrometers which accelerate or retard the scattered electrons to the same energy before analysis. We have used a commercial double-pass cylindrical-mirror electron spectrometer with spherical retarding grids at the input.[17] The spectrometer was run in the retarding mode with a pass energy $E_{pass}$ of 50 eV. This gave a spectrometer resolution of about 0.4 eV, indepenent of the electron energy being analyzed. The one parameter that varies with electron energy in this type of spectrometer is the area of the sample that is "seen" by the spectrometer. This area varies as $(E_{pass}/E)^{1/2}$, where $E$ is the electron energy being analyzed, so the area decreases with increasing electron energy. This is only a problem when trying to compare the absolute amplitudes of loss spectra taken at different incident energies, or when the energy range of the loss spectrum is comparable to the incident energy; neither of those cases will be considered here.

The energy profile of the incident electron beam is more difficult to control. Our spectra were excited with the electron gun in, and coaxial with, the spectrometer. This gun was a conventional design utilizing a $W$ cathode with no additional energy selection. It was necessary to reduce the cathode temperature at higher energies in order to keep the energy profile of the beam as narrow as at low energies (0.2 mA total filament emission at $E_p = 2000$ eV, compared to 2.0 mA at 100 eV). Even then it was impossible to get precisely the same profile at all energies; the tail on the low-energy side of the beam was broader at high energies than at low energies. We did, however, set the full width at half maximum (FWHM) of the beam to be the same at all energies (about 0.4 eV). In this way the system resolution was independent of energy, and the only effect of the broader tail at high energies was to make it slightly more difficult to resolve loss features close to the elastic peak. A modulation voltage of 0.4 eV peak to peak was applied to the beam voltage rather than to the spectrometer in order to eliminate Auger peaks from the spectrum. The resultant system resolution was about 0.7 eV.

The energy-loss spectra were recorded as the first derivative of the emitted electron distribution, $dn(E)/dE$, versus energy loss $E_L$. Peaks in $n(E)$ thus correspond to midpoints of negative slopes in $dn(E)/dE$ (or maximum negative slopes or zero crossings, depending on the details of peak shape and background slope). We use the first derivative of $n(E)$ rather than the second derivative, which is often used, to avoid spurious features in the loss spectra.[18] Unless noted, the energy-loss spectra were taken with the incident beam normal to the sample surface. Some spectra were also taken with the incident beam at grazing incidence in order to sample as little of the bulk as possible; where no angle is specified for grazing-incidence spectra, the electron beam was incident within 2° or less of the surface plane.

The MgO samples used were (100) faces that were cleaved from a single crystal in air, polished with 0.5-$\mu$m diamond paste to remove cleavage steps, and etched for 30 sec in boiling $H_3PO_4$. After mounting in the ultrahigh-vacuum system, they were Ar-ion sputter-etched at 500 eV and then annealed at about 1400 K for a few minutes by electron bombardment. The resulting surface yielded excellent LEED patterns,[19] which were slightly better than those from vacuum-cleaved surfaces.

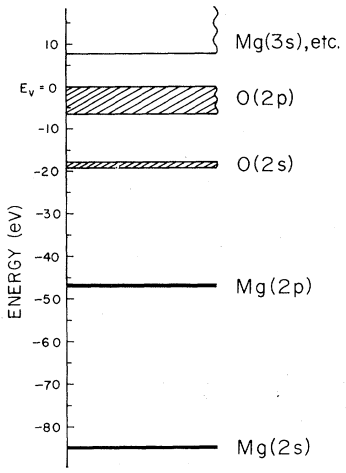


FIG. 2. Schematic energy-level diagram for MgO.

Auger spectroscopy showed the surfaces to be atomically clean. Energy-loss spectra obtained from surfaces prepared in the above manner were indistinguishable from those for vacuum-cleaved surfaces, with the exception of one peak to be discussed in Sec. VI.

## IV. CORE-LEVEL ENERGY-LOSS SPECTRA

An approximate energy-level diagram for MgO, based primarily on XPS measurements,[20] is given in Fig. 2. Figure 3 shows the energy-loss spectrum of MgO (100) for $0 < E_L < 110$ eV, taken with $E_p = 200$ eV. For $E_L \gtrsim 50$ eV, the structure arises predominantly from intraionic transitions on Mg ions, while the spectrum for $E_L \lesssim 50$ eV consists of plasma losses, intraionic transition on O ions, and interionic (O-to-Mg) transitions. We will

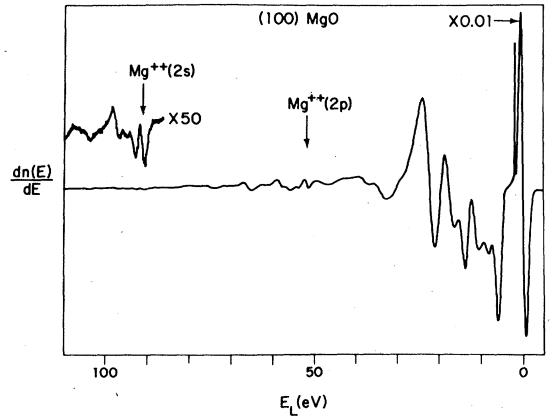


FIG. 3. Electron-energy-loss spectrum, $dn(E)/dE$ vs $E_L$, for MgO (100) with $E_p = 200$ eV. Arrows indicate thresholds for excitation from the $Mg^{2+}$ $2p$ and $Mg^{2+}$ $2s$ core levels.

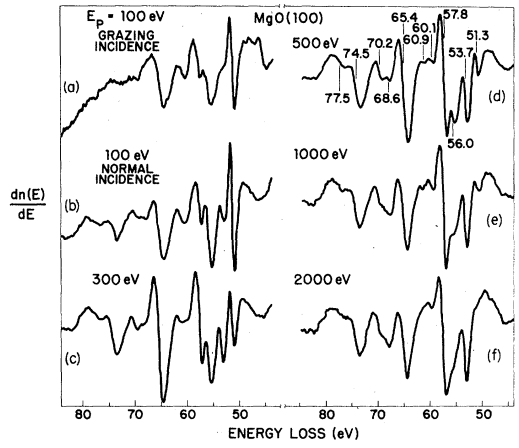


FIG. 4. Energy-loss spectra, $dn(E)/dE$ vs $E_L$, for transitions from the Mg $2p$ core level in MgO for 100 eV $\leq E_p \leq 2000$ eV.

discuss the Mg intraionic transitions in this section and the plasmon and interionic excitations in Sec. V.

### A. Separation of surface and bulk transitions

Transitions from the Mg $2p$ core level to empty states above the Fermi level begin at $E_L \approx 51$ eV

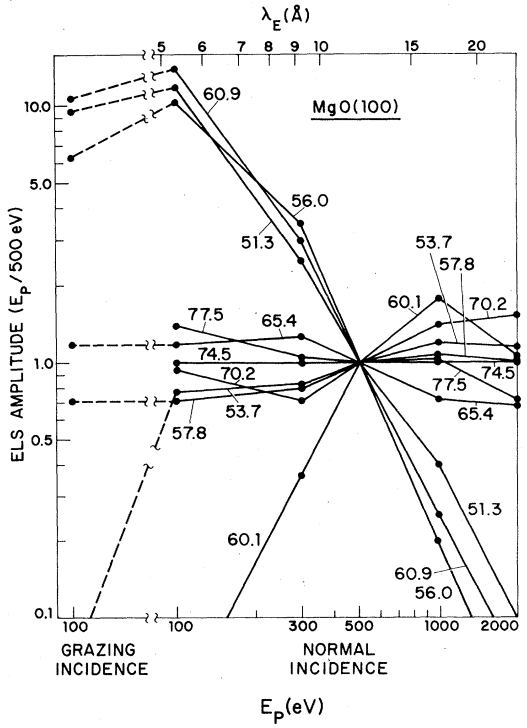


FIG. 5. Peak-to-peak amplitude of peaks in energy-loss spectra of Fig. 4 versus $E_p$, normalized at $E_p = 500$ eV. Numbers labeling curves indicate loss energy in eV.

and extend to $E_L \approx 80$ eV.[8,21] Similar transitions from the Mg 2$s$ core level to the same final states begin at $E_L \approx 93$ eV. The widths of both the Mg 2$p$ and Mg 2$s$ initial states (< 0.3 eV) are smaller than our resolution, so the structure observed for transitions from those levels will be due to the density of final states.

Figures 4(b)–4(f) show the energy-loss spectra for Mg 2$p$-to-excited-state transitions for $120 \leq E_p \leq 2000$ eV, normal incidence. Figure 4(a) shows the loss spectrum taken at $E_p = 120$ eV and grazing incidence. The loss energies of peaks in $n(E)$ are given in Fig. 4(d). The most striking feature of these spectra is the large change in the relative amplitudes of the peaks as a function of primary-electron energy. The peaks at 51.3 and 56.0 eV are very large for $E_p = 120$ eV, both normal and grazing incidence, and decrease with increasing $E_p$ until they are merely shoulders at $E_p = 2000$ eV. The 53.7- and 57.8-eV peaks, on the contrary, are largest for $E_p = 2000$ eV and decrease with decreasing $E_p$; at $E_p = 120$ eV, grazing incidence, the 53.7-eV peak has completely disappeared. The rest of the peaks, with the exception of the one at 60.1 eV, remain roughly constant for all values of $E_p$.

These changes can be seen more clearly in Fig. 5, where the relative amplitude of the peaks [i.e., the peak-to-peak amplitdue in $dn(E)/dE$] is plotted versus $E_p$. No attempt was made to determine the change in absolute amplitude of the peaks at different $E_p$ for the reasons discussed in Secs. II and III above. Instead, the data were normalized to the sum of the amplitudes of those peaks whose relative amplitudes remained fairly constant for different $E_p$. The normalized amplitude of each peak was then divided by its value at 500 eV to generate the ordinate in Fig. 5. The average mean free path for electrons of energy $E_p$, taken from the dashed curve in Fig. 1, is given along the top of the figure. The data for $E_p = 120$ eV, grazing incidence, cannot really be plotted on the abscissa of Fig. 5, but since they represent a very shallow penetration into the sample they have been included at the left of the figure.

The three energy-loss peaks at 51.3, 56.0, and 60.9 eV arise from electronic transitions involving surface ions. The remaining features, except for the 60.1-eV peak that will be discussed in Sec. IV B below, vary in amplitude by a factor of 2 or less for $120 \leq E_p \leq 2000$ eV, indicating that they are of bulk origin. The variation in amplitude with $E_p$ is small enough to arise from differences in the energy dependence of the excitation probability for the transitions (Sec. II A). The disappearance of the peaks at 53.7, 70.2, 74.5, and 77.5 eV at $E_p = 120$ eV, grazing incidence, suggests that we are no longer sampling bulk ions. The two peaks at 57.8 and 65.4 eV, which were identified as being of bulk origin from the normal-incidence spectra, do not disappear at grazing incidence. Since the other bulk peaks have disappeared, however, we assume that surface transitions exist that are nearly degenerate with the bulk transitions at those energies; this will be discussed in Sec. IV C below.

### B. Origin of bulk transitions

We have previously discussed the origin of the bulk transitions that involve the Mg 2$p$ and Mg 2$s$ core levels in Refs. 8 and 21; we will only summarize that work here for completeness. The bulk energy-loss structure involving the Mg 2$p$ core level begins abruptly with the peak at $E_L = 53.7$ eV and continues until $E_L \approx 80$ eV. The next bulk structure, due to transitions from the Mg 2$s$ core level, begins at $E_L = 93.1$ eV and continues until $E_L \approx 120$ eV. When the Mg 2$s$ loss spectrum is shifted 39.4 eV to lower loss energy, it is almost identical to the Mg 2$p$ spectrum (with the exception of one peak to be discussed in Sec. IV C below), confirming that both spectra arise from structure in the density of final states.

MgO is a highly ionic compound consisting of $Mg^{2+}$ and $O^{2-}$ ions.[22] It is thus reasonable to compare the energy-loss spectra with optical excitation spectra for free $Mg^{2+}$ ions. This has been done in Fig. 6, where the Mg 2$p$ energy-loss spectrum is plotted in (a) and a histogram of the observed optical transitions from the Mg 2$p$ ground state to excited states is plotted in (b). The tran-

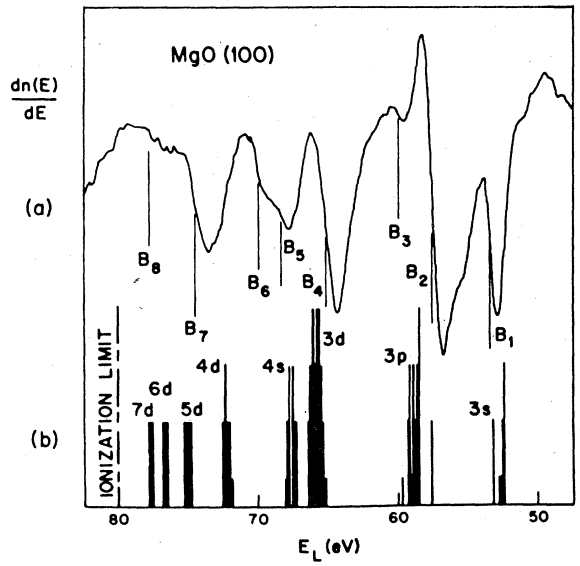


FIG. 6. (a) Energy-loss spectra, $dn(E)/dE$ vs $E_L$, for excitations from the Mg 2$p$ core level in MgO for $E_p = 2000$ eV; (b) observed $Mg^{2+}$ free-ion spectrum from Ref. 23.

sition energies in Fig. 6(b) are taken from Ref. 23, and the ordinate is proportional to the multiplicity of the excited states. The 53.7, 57.8, 65.4, and 70.2 eV loss peaks lie very close to the 3*s*, 3*p*, 3*d*, and 4*s* levels, respectively, in the $Mg^{2+}\,2p \rightarrow nl$ series in Fig. 6(b). Additional peaks in the energy-loss spectrum are seen up to the ionization limit of the free $Mg^{2+}$ ion, with no further structure until the onset of the Mg 2*s* spectrum. It thus appears that the $Mg^{2+}$ ions in MgO behave very nearly like free $Mg^{2+}$ ions.

Calculations of the electronic structure of MgO have been made using the itinerant-electron (energy-band) formalism,[24,25] and we have also compared our data to the conduction-band density of states from one of those calculations.[24] The calculation changes the order of many of the excited states relative to the free ion, and the resulting conduction-band density of states is entirely different from the observed free-ion levels [Fig. 6(b)]. Our data are in poor agreement with the band calculations, indicating that the localized electron (ionic) limit yields a better description of the electronic excitation spectrum on the $Mg^{2+}$ ions in MgO.

The energy-loss peak at 60.1 eV, which only exists for $E_p \geq 300$ eV, does not fit the criteria for either a bulk or a surface intraionic transition. The fact that its amplitude increases with $E_p$ relative to single-bulk-loss features raises the possibility that it might correspond to a multiple- (presumably double) loss process. The lowest-energy double-loss process in that energy range involving only bulk transitions would be the excitation of a $Mg^{2+}$ intraionic transition (53.7 eV) and an interionic O-to-Mg transition (8.2 eV, see Sec. V below), which would result in a loss energy near 61.9 eV. The observed energy loss could be more closely approximated by the excitation of one bulk and one surface transition, either a surface $Mg^{2+}$ excitonic (51.3 eV) and a bulk interionic (8.2 eV) transition, resulting in a loss at 59.5 eV, or a bulk $Mg^{2+}$ transition (53.7 eV) and a surface interionic transition (6.2 eV), resulting in $E_L = 59.9$ eV. At the present time we do not have enough information to definitively identify the origin of that peak.

### C. Stark-effect model of surface ionic levels

We have previously published an interpretation of the origin of the surface features in the Mg 2*p* and Mg 2*s* core-level energy-loss spectra of MgO (100),[8] and we will only review it briefly here. The success of the free-ion picture in interpreting the bulk energy-loss spectra from those levels suggests that an ionic description should also be applicable to surface transitions. There is a large change in Madelung potential at the surface due to the termination of the crystal. This potential should be approximately the same for initial and final states of the $Mg^{2+}$ ion in an energy-loss experiment and should therefore nearly cancel out. There is in addition a large gradient in the Madelung potential at the surface of an ionic insulator, which would give rise to a strong electric field that should produce a Stark mixing of ionic states. We have applied a simple model of this effect to calculate the Stark-split spectrum of $Mg^{2+}$ surface ions.

In our model, we assume no relaxation or reconstruction of the surface so that all surface ions have the same positions that they would have in the bulk. We then assume that an average electric field $\vec{\mathcal{E}}_s$, normal to the surface, at the position of a surface $Mg^{2+}$ ion produces a Stark interaction term $\mathcal{H}_{\text{Stark}} = -e\vec{\mathcal{E}}_s \cdot \vec{r}$. We consider only the contributions of the 3*s*, 3*p*, 3*d*, 4*s*, 4*p*, 4*d*, and 4*f* ionic levels, and we take their values at zero electric field from the experimentally determined bulk transitions. We then use a hydrogenic model for the Stark shift and calculate the position of the excited ionic levels as a function $\mathcal{E}_s$. (For a more detailed description of the procedure, see Ref. 8.)

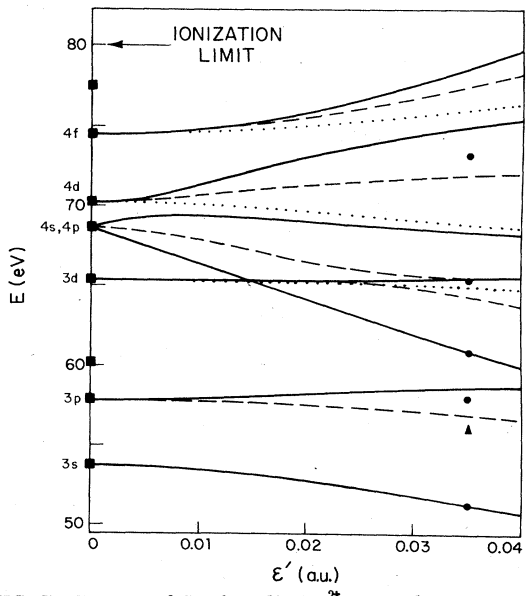


FIG. 7. Energy of Stark-split $Mg^{2+}$ excited states versus normalized surface electric field $\mathcal{E}'$ (in atomic units). Full lines represent $m_l = 0$ levels, dashed lines are $m_l = \pm 1$ levels, and dotted lines are $m_l = \pm 2$ levels. The $m_l = \pm 3$ level associated with 4*f* is not shown. Squares are observed bulk peaks; dots and triangle are observed surface peaks. The triangular point is inferred to be an $m_l = \pm 1$ level in view of the selection rule discussed in the text.

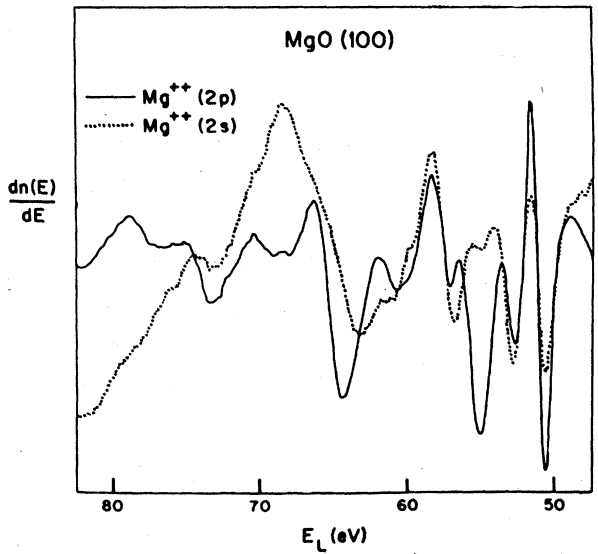


FIG. 8. Energy-loss spectra, $dn(E)/dE$ vs $E_L$, for transitions from the Mg $2p$ (solid curve) and Mg $2s$ (dotted curve) core levels in MgO for $F_p = 100$ eV, normal incidence.

The results of the calculation are given in Fig. 7, where $\mathcal{E}'$ is the electric field expressed in atomic units (a.u.). The experimentally determined energies of the surface transitions (circles and triangle) were then positioned in $\mathcal{E}'$ to give the best overall fit. This resulted in a value of $\mathcal{E}' \cong 0.053$ a.u., corresponding to a surface electric field $\mathcal{E}_s \cong 2.9 \times 10^8$ V/cm. This is reasonably close to the value of $\mathcal{E}_s \cong 1.9 \times 10^8$ V/cm calculated for the Madelung electric field at the center of a $Mg^{2+}$ ion on the unrelaxed (100) surface of MgO.

The presence of strong electric fields at the surface would be expected to drive some reconstruction of the first atomic layer.[26] Recently, Martin and Bilz[27] have performed shell-model calculations of the structure of the MgO (100) surface. They find that a surface in which the Mg ions relax inward by 3.4% of the bulk interionic distance $a$, while the O ions do not relax but polarize by about 3% of $a$, agrees with LEED measurements[28] of the structure of MgO (100). The surface ions in that model[27] are found to be about 5% *more* ionic than the bulk ions. That results in a 30% *increase* in the surface electric field, compared to the 50% increase determined from our Stark model.

Additional evidence for the Stark-effect model of the surface states is given by the Mg $2s$-to-excited-state energy-loss spectra. Figure 8 shows the 100-eV normal-incidence spectra for transitions from the Mg $2p$ (solid line) and Mg $2s$ (dotted line) core levels. The Mg $2s$ spectrum has been shifted by 39.4 eV to align it with the Mg $2p$ spectrum. The two spectra are similar, indicating transitions to the same excited states, except that the second surface peak (at 56.0 eV in the Mg $2p$ spectrum) is much smaller in the Mg $2s$ spectrum; this is the peak represented by the triangle in Fig. 7. Because the interaction of the $Mg^{2+}$ surface ion with a normally incident electron beam has cylindrical symmetry, the resulting transitions should have $\Delta m_l = 0$ (assuming small-angle scattering) so that the $(2s, m_l = 0) \rightarrow (nl, m_l = \pm 1)$ transitions would be forbidden. The surface transition represented by the triangle in Fig. 7 is the only one of the first five whose final state is $m_l = 1$, so it should be allowed from the Mg $2p$ level ($m_l = 0, \pm 1$) but forbidden from the Mg $2s$ level ($m_l = 0$), as observed. When the electron beam is tipped away from normal incidence, the $\Delta m_l = 0$ selection rule breaks down. We do, in fact, see more than a tenfold increase in the relative amplitude of that peak in the Mg $2s$ spectrum when the electron beam is moved toward grazing incidence.

Although the experimental data are suggestive of a surface Stark effect, conceptual difficulties remain. For an effective charge of 3, a rough hydrogenic value for the size of the $Mg^{2+}$ ($n = 3$) orbit is ~2.25 Å. Since the distance between the $Mg^{2+}$ and the $O^{2-}$ ions in MgO is only 2.1 Å, there would be a large overlap of the $Mg^{2+}$ ($n = 3$) orbit and the $O^{2-}$ charge cloud, suggesting the importance of banding. Nevertheless, as demonstrated in Refs. 8 and 21, we have found the Mg core-level excitonic states in MgO to be in poor agreement with the conventional itinerant-electron band picture of MgO.

## V. INTERIONIC TRANSITIONS AND PLASMA LOSSES

For $E_L \lesssim 50$ eV, it is not possible to excite intraionic transitions on the Mg ions. The spectra in this region must arise from O intraionic transitions, O-to-Mg interionic transitions, and the excitation of plasma oscillations. The energy-loss spectra for $E_L \lesssim 30$ eV are shown in Fig. 9; the region $30 < E_L < 50$ eV exhibits only two relatively weak features, and we will not consider it here. Fugures 9(b)–(f) give the spectra for $E_p = 100$ to 2000 eV normal incidence and Fig. 9(a) gives the spectrum for $E_p = 100$ eV grazing incidence. The peak-to-peak amplitudes of the features in these spectra versus primary energy, normalized in the same way as for the core-level energy-loss spectra, are plotted in Fig. 10. Primary-electron-energy-dependent effects are

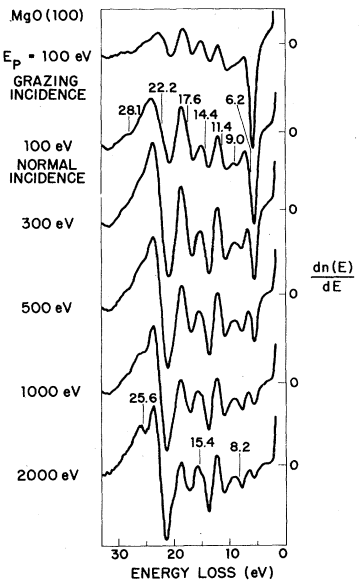


FIG. 9. Energy-loss spectra, $dn(E)/dE$ vs $E_L$, for MgO (100) for 100 eV $\leq E_p \leq$ 2000 eV.

not as striking here as in the Mg core-level spectra, but there are three peaks whose amplitudes change significantly with energy. The lowest-energy peak, at 6.2 eV, is extremely strong at low energies and at grazing incidence, decreasing an order of magnitude by 2000 eV. We hence identify it as a surface transition. It could not be a bulk transition in any event since its energy is less than the 7.77-eV band gap in MgO.[29] The peak at 22.2 eV is relatively constant in amplitude for $300 \leq E_L \leq 2000$ eV, but it decreases by a factor of 4 on going to grazing incidence. This peak has been identified as the bulk plasma oscillation corresponding to collective oscillation of all of the electrons in the O 2$p$ valence band[29,30]; its energy is indeed close to the value of 22.7 eV calculated in the free-electron approximation.

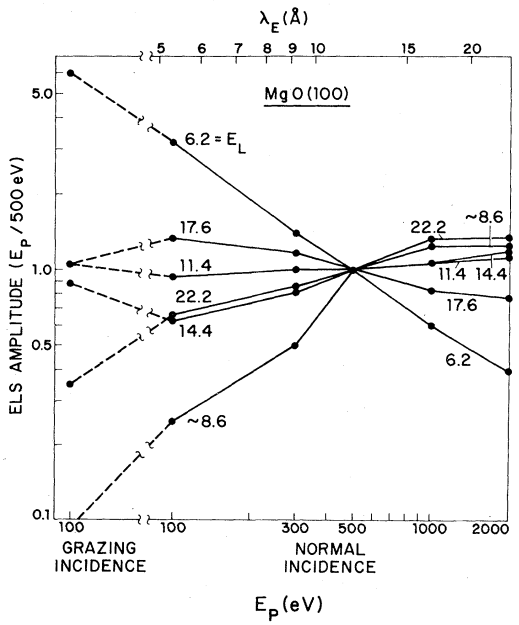


FIG. 10. Peak-to-peak amplitude of peaks in energy-loss spectra of Fig. 9 versus $E_p$, normalized at $E_p$=500 eV. Numbers labeling curves indicate loss energy in eV.

The peak at 8.2 eV in the 2000-eV spectrum decreases in amplitude below $E_p$=300 eV, virtually disappearing in the grazing incidence spectrum. It corresponds to excitation of electrons from the O 2$p$ band to the Mg 3$s$ levels, presumably from peaks in the respective densities of states near the band edges. (Its energy is close to the fundamental optical absorption edge at 7.77 eV.) Its disappearance in surface-sensitive spectra, coupled with the attendant increase in intensity of the 6.2-eV peak, suggests that the lowest 3$s$ states on the surface Mg ions are shifted about 2 eV toward larger binding energy relative to the bulk ions. The data could also be explained by a decrease in the binding energy of the states near the top of the O 2$p$ valence band. However, the fact that a 2-eV shift of the lowest-lying Mg final states is also seen in the Mg core-level loss spectra makes that explanation unlikely.

High-energy transmission-energy-loss measurements on thin MgO samples have been made by von Festenberg[31] and by Venghaus[30]; the location of our energy-loss peaks for $E_L \leq 30$ eV are in agreement with theirs except that they do not observe the 6.2-eV surface loss peak. We cannot make a more detailed comparison of our data with theirs since we have measured $dn(E)/dE$ rather than $n(E)$.

The location of peaks in our energy-loss spectrum for $E_p$=2000 eV are compared with Im$(-1/\mathcal{E})$ computed by Roessler and Walker[29] from their ultraviolet reflectance measurements on MgO in Fig. 11. The agreement in peak location is good except, of course, for the surface loss peak at 6.2 eV. Calculations of the bulk band structure of MgO have been made by Fong *et al.*[32] and by Pantelides *et al.*[24] The agreement between $\mathcal{E}_1$, $\mathcal{E}_2$, and Im$(-1/\mathcal{E})$ from those calculations and the data of Roessler and Walker is fairly good. We thus conclude that the O-to-Mg energy-loss spectra are in basic agreement with energy-band calculations for MgO. This is in contrast to the Mg core-level energy-loss excitation spectra, which do not agree with itinerant-electron calculations for the Mg conduction band. This difference no doubt arises from the highly localized nature of the excitonic core-level transitions as compared

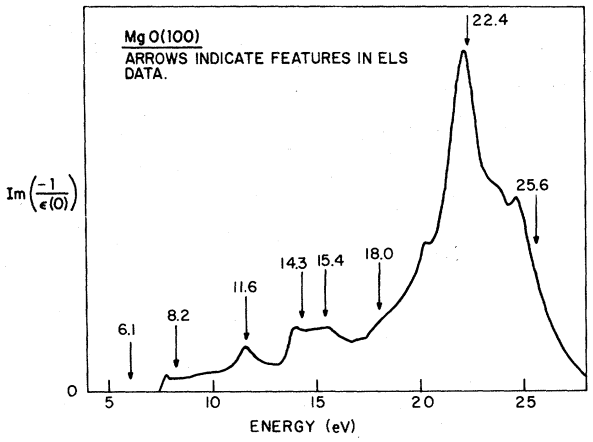


FIG. 11. Energy-loss function for MgO computed from dielectric-constant measurements of Roessler and Walker (Ref. 29). Arrows indicate location of energy-loss peaks observed in this work.

to the more spatially diffuse O-to-Mg transitions that involve initial and final states on two different ions. The fact that the 6.2-eV surface loss peak does not completely disappear for $E_p = 2000$ eV, while the 51.3-eV surface-state peak does, is consistent with the different degree of final-state localization in the two cases.

The surface electronic structure of MgO has been considered by two groups. Lee and Wong[33] have performed both Green's function and linear combination of atomic orbitals (LCAO) calculations of the surface energy-band structure of MgO. For MgO (100), they find a surface-state band that extends about 0.5 eV above the top of the bulk O $2p$ valence band, while the Mg $3s$ surface band lies entirely above the bulk conduction-band minimum (which occurs at $\Gamma$). No direct transitions involving surface states exist in their calculation with energies less than 7.6 eV; the lowest-energy indirect transition (from $X$ in the O $2p$ band to $\Gamma$ in the Mg $3s$ band) would be at about 7.3 eV. Their calculation thus cannot account for the observed loss peak at 6.2 eV.

Satoko *et al.*[34] have performed discrete variational $X\alpha$ cluster calculations for both bulk and surface MgO clusters. Using both $(MgO_5)^{8-}$ and $Mg_9O_9$ surface clusters, they find that a peak in the surface density of states occurs 2 eV below the bottom of the bulk Mg $3s$ conduction band, in agreement with our data. In those calculations the 2-eV shift results from a balance between a reduction in the Madelung potential near the surface, differences between cation-anion charge transfer for surface and bulk ions, and polarization of the wave functions of the surface ions due to the potential gradient at the surface. The first and third of these are included in the Stark-effect description in Sec. IV and in Ref. 8.

## VI. DEFECT SURFACE STATES ON MgO

The above energy-loss spectra are seen on vacuum-cleaved MgO (100) surfaces, on surfaces that have been sputtered and annealed in vaccum, and even on surfaces that have only been sputtered; the spectra are essentially independent of surface preparation. This is not too surprising in view of the extreme stability of the MgO (100) surface.[19] There is one additional energy-loss peak, however, that is very sensitive to surface treatment. Figure 12 shows the energy-loss spectra for a sample that was sputtered, annealed, and then bombarded with 1000-eV electrons for about 30 min. The spectra for all primary energies are essentially indistinguishable from those in Fig. 9 for a surface that had not been subjected to electron bombardment, except for the presence of a large loss peak at about 2.3 eV. (The true location of that peak may in fact be at a slightly smaller loss energy than 2.3 eV due to interference from the elastically reflected beam.) The amplitude of the 2.3-eV loss peak as a function of $E_p$ parallels that of the 6.2-eV loss peak, indicating that it is of surface origin. (There is an additional complication due to the slight broadening of the elastic peak at large $E_p$ mentioned in Sec. III, but that is not enough to cause the observed decrease in amplitude of the 2.3-eV peak.) The surface nature of this loss peak can also be demonstrated by its behavior upon exposure to $O_2$, as shown in Fig. 13 for $E_p = 100$ eV, normal

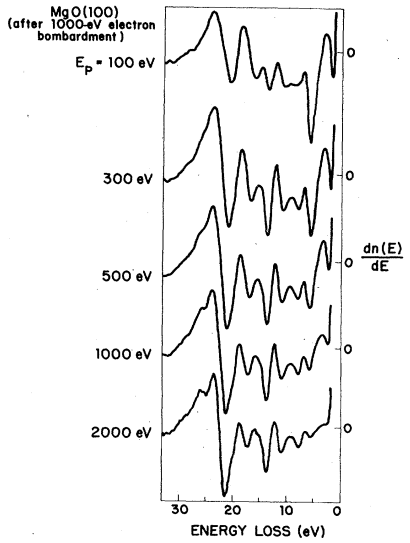


FIG. 12. Energy-loss spectra, $dn(E)/dE$, for MgO (100) after 30-min exposure to 1000-eV electron beam.

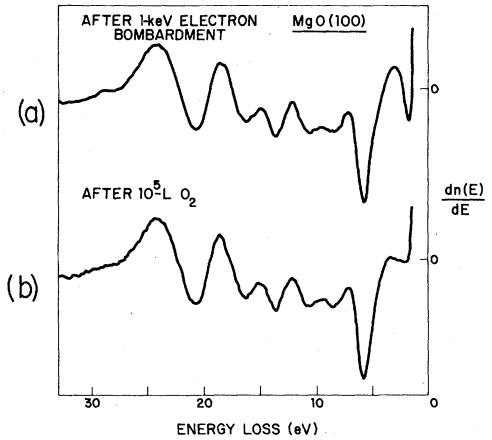


FIG. 13. Energy-loss spectra for electron-bombarded MgO (a) before and (b) after exposure to $10^5$-langmuir $O_2$. $E_p = 100$ eV.

incidence. Exposure to $10^5$ langmuir of $O_2$ produces no changes in the loss spectra except for the virtual elimination of the 2.3-eV peak. The amplitude of the low-energy-loss peak varies from measurement to measurement, and it is sometimes present on sputtered surfaces that have not been exposed to electron bombardment.

The fact that the amplitude of the 2.3-eV transition depends in some manner on ion or electron bombardment suggests that it may be associated with surface defects. Similar loss peaks have been seen on $TiO_2$ (Ref. 35) and $SrTiO_3$ (Ref. 36) and are associated with surface O vacancies. The microscopic nature of the defect sites is thought to be different in those two cases, however.

It is tempting to attribute the loss peak to a simple surface $F$ center, $F_s^+$, consisting of one electron trapped at a surface O vacancy, which has been observed by spin-resonance techniques.[37] Recent calculations by Kassim *et al.*,[38] however, show that the transition energy of such a center should be close to that of the bulk $F^+$ center, about 5 eV. Nelson and Hale[39] have observed a band at 2.1 eV in diffuse reflectance spectra from MgO powders after $\gamma$ irradiation in vacuum, but that state could have originated on crystal faces other than (100).

Recent preliminary results[40] on vacuum-cleaved MgO (100) surfaces show that the low-energy-loss peak is also present on some cleaved surfaces that exhibit very good LEED patterns. The origin of that loss peak is not clear at this time, and additional work is currently underway.

## ACKNOWLEDGMENTS

The authors are pleased to acknowledge numerous extremely helpful discussions with V. M. Bermudez and V. H. Ritz, and the technical assistance of B. Feldman. This work was sponsored by the Department of the Air Force.

*Present address: Department of Engineering and Applied Science, Yale University, New Haven, Connecticut 06520.

†Present address: Francis Bitter National Magnet Laboratory, MIT, Cambridge, Massachusetts 02139.

[1]E. Rudberg, Proc. R. Soc. London Ser. A 127, 111 (1930); Phys. Rev. 50, 138 (1936).

[2]R. Ludeke and A. Koma, Phys. Rev. Lett. 34, 817 (1975).

[3]J. J. Ritsko, L. J. Brillson, and D. J. Sandman, Solid State Commun. 24, 109 (1977).

[4]G. W. Rubloff, Solid State Commun. 26, 523 (1978).

[5]See, for example, C. C. Chang, Surf. Sci. 48, 9 (1975).

[6]C. J. Powell and J. B. Swan, Phys. Rev. 115, 869 (1959).

[7]See, for example, P. E. Best, Proc. Phys. Soc. London 79, 133 (1962); E. J. Scheibner and L. N. Tharp, Surf. Sci. 8, 247 (1967); J. Hölzl, H. Mayer, and K. W. Hoffman, *ibid.* 17, 232 (1969); A. Adnot, Y. Ballu, and J. D. Carette, J. Appl. Phys. 43, 693 (1972); H. Froitzheim, in *Electron Spectroscopy for Surface Analysis*, edited by H. Ibach (Springer, Berlin, 1977), p. 205.

[8]V. E. Henrich, G. Dresselhaus, and H. J. Zeiger, Phys. Rev. Lett. 36, 158 (1976); *ibid.* 38, 872(E) (1977).

[9]H. Raether, Springer Tracts in Mod. Phys. 38, 84 (1965).

[10]A. A. Lucas and M. Šunjić, Prog. Surf. Sci. 2, 75 (1972).

[11]H. S. W. Massey and E. H. S. Burhop, *Electronic and Ionic Impact Phenomena* (Clarendon, Oxford, 1969), Vol. I.

[12]H. S. W. Massey and E. H. S. Burhop, *Electronic and Ionic Impact Phenomena* (Clarendon, Oxford, 1969), Vol. II.

[13]C. J. Powell, Surf. Sci. 44, 29 (1974).

[14]D. M. Smith, T. E. Gallon, and J. A. D. Matthew, J. Phys. B 7, 1255 (1974).

[15]R. H. Ritchie, Phys. Rev. 106, 874 (1957); R. A. Ferrell and J. J. Quinn, *ibid.* 108, 570 (1957); G. D. Mahan, Phys. Status Solidi B 55, 703 (1973).

[16]P. J. Feibelman, Surf. Sci. 36, 558 (1973).

[17]Physical Electronics Model 15-255G Double-Pass Cylindrical Mirror Electron Spectrometer.

[18]V. E. Henrich, Appl. Surf. Sci. (in press).

[19]V. E. Henrich, Surf. Sci. 57, 385 (1976).

[20]S. P. Kowalczyk, F. R. McFeely, L. Ley, V. T. Gritsyna, and D. A. Shirley, Solid State Commun. 23, 161 (1977).

[21]V. E. Henrich and G. Dresselhaus, Solid State Commun. 16, 1117 (1975).

[22]P. M. Raccah and R. J. Arnott, Phys. Rev. 153, 1028 (1967).

[23]C. E. Moore, *Atomic Energy Levels*, Natl. Bur. Stds. (U.S.) Circ. No. 467 (U. S. GPO, Washington, D. C., 1949), Vol. I.
[24]S. T. Pantelides, D. J. Mikish, and A. B. Kunz, Phys. Rev. B 10, 5203 (1974).
[25]N. Daude, C. Jouanin, and C. Gout, Phys. Rev. B 15, 2399 (1977).
[26]H. A. Kassim and J. A. D. Matthew, Surf. Sci. 65, 443 (1977).
[27]A. J. Martin and H. Bilz, Phys. Rev. B 19, 6593 (1979).
[28]M. R. Welton-Cook and M. Prutton, Surf. Sci. 74, 276 (1978).
[29]D. M. Roessler and W. C. Walker, Phys. Rev. 159, 733 (1967).
[30]H. Venghaus, Op. Commun. 2, 447 (1971).
[31]Cited in Ref. 29 above.
[32]C. Y. Fong, W. Saslow, and M. L. Cohen, Phys. Rev. 168, 992 (1968).
[33]V.-C. Lee and H.-S. Wong, J. Phys. Soc. Jpn. 45, 895 (1978).
[34]C. Satoko, M. Tsukada, and H. Adachi, J. Phys. Soc. Jpn. 45, 1333 (1978).
[35]V. E. Henrich, G. Dresselhaus, and H. J. Zeiger, Phys. Rev. Lett. 36, 1335 (1976).
[36]V. E. Henrich, G. Dresselhaus, and H. J. Zeiger, Phys. Rev. B 17, 4908 (1978).
[37]For a summary of bulk defects in MgO, see A. E. Hughes and B. Henderson, in *Point Defects in Solids*, edited by J. H. Crawford, Jr., and L. M. Slifkin (Plenum, New York, 1972), Vol. I, p. 381.
[38]H. A. Kassim, J. A. D. Matthew, and B. Green, Surf. Sci. 74, 109 (1978).
[39]R. L. Nelson and J. W. Hale, Discuss. Faraday Soc. 52, 77 (1971).
[40]V. E. Henrich and R. L. Kurtz, Fortieth Annual Conference on Physical Electronics, Cornell University, 1980 (unpublished).